

Supporting Information

Effect of Solvent Hydrophobicity on Gelation Kinetics and Phase Diagram of Gelatin Ionogels

Kamla Rawat¹, Jyotsana Pathak¹ and H.B.Bohidar^{1,2*}

¹Polymer and Biophysics Laboratory, School of Physical Sciences,

²Special Center for Nanosciences, Jawaharlal Nehru University, New Delhi 110067, India

*Corresponding author email: bohi0700@mail.jnu.ac.in

Tel: +91 11 2670 4637, Fax: +91 11 2674 1837

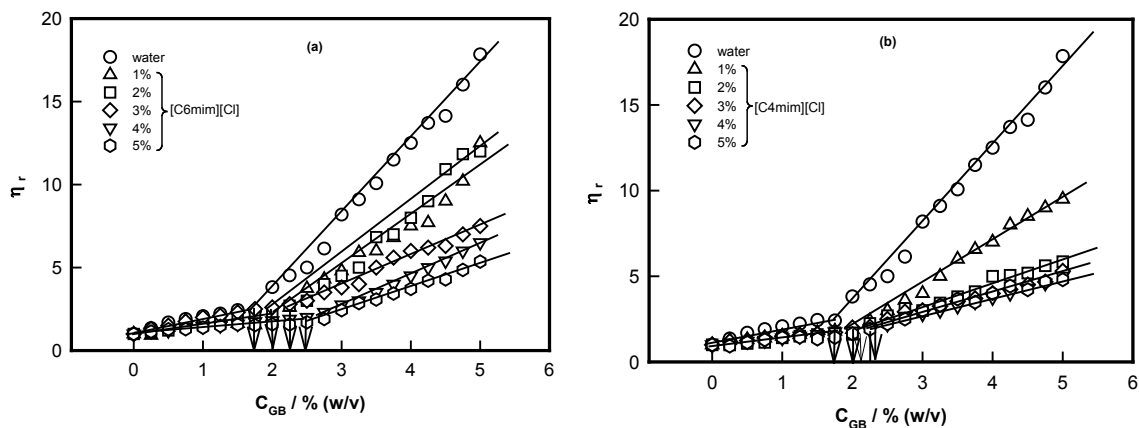


Figure S1: c_g profile of gelatin B in different a) [C6mim][Cl] and b) [C4mim][Cl] solutions. Standard deviations in the reported η values are ± 2 mPa s.

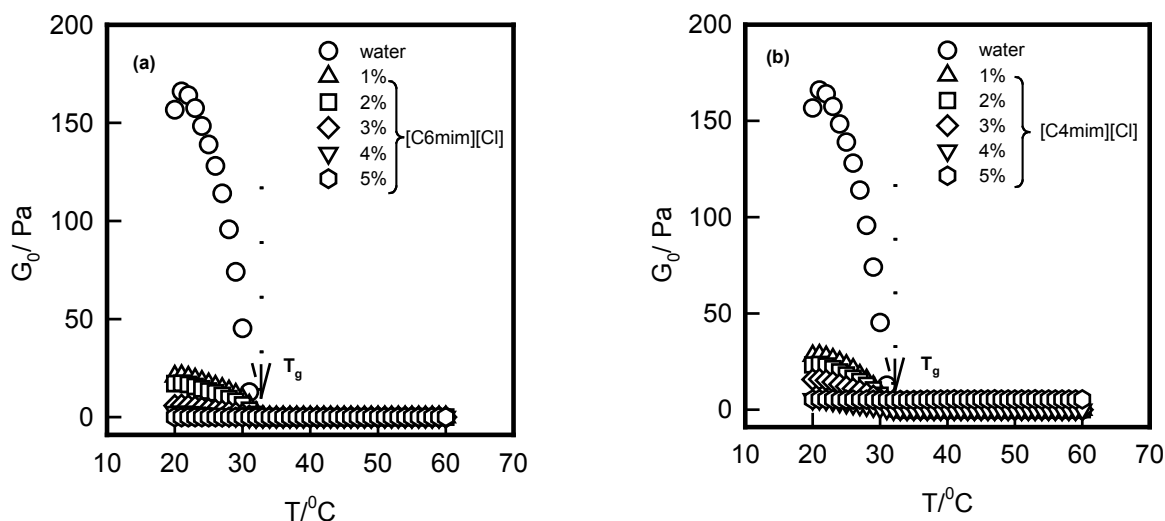


Figure S2: Variation of storage modulus profile for a) [C6mim][Cl] and b) [C4mim][Cl] based ionogels (5% gelatin B) as a function of temperature. Arrows represent the indicative melting temperature T_g . Standard deviations in the reported G_0 and T values are ± 2 Pa and ± 0.5 °C.

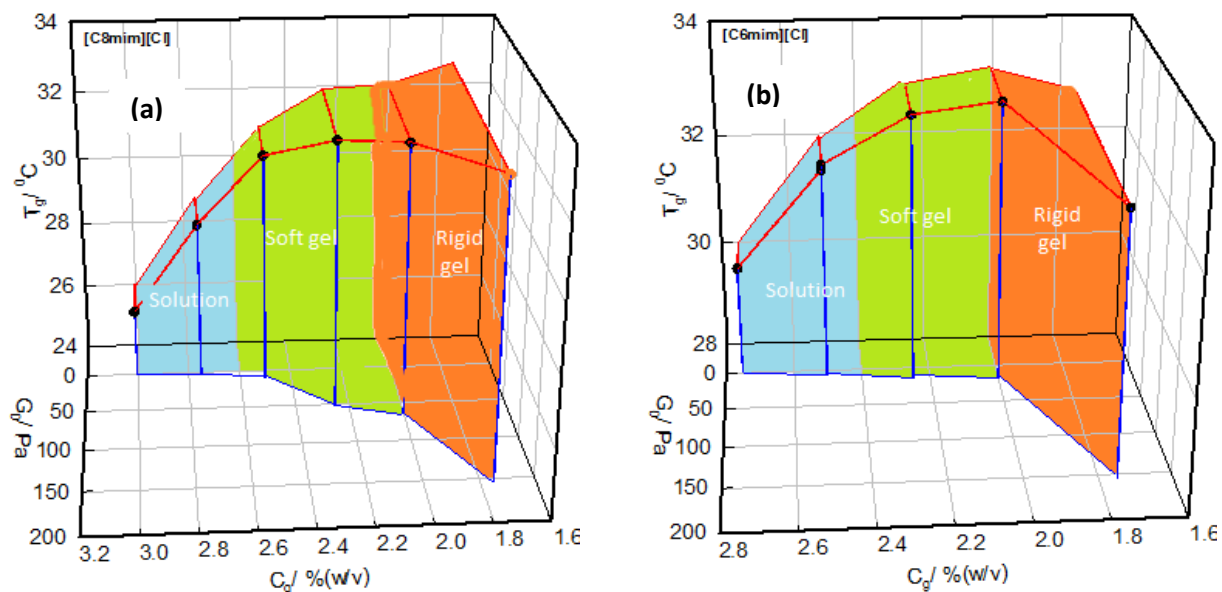


Figure S3: 3D phase diagram of gelatin B ionogel in a) [C8mim][Cl] and b) [C6mim][Cl] solution. Note that the gelation concentration increases, and gelation temperature reduces and network rigidity decreases, when IL concentration is increased in the solvent. Standard deviations in the reported c_g , T and G_0 values are ± 0.1 % (w/v), ± 0.5 °C and ± 2 Pa.

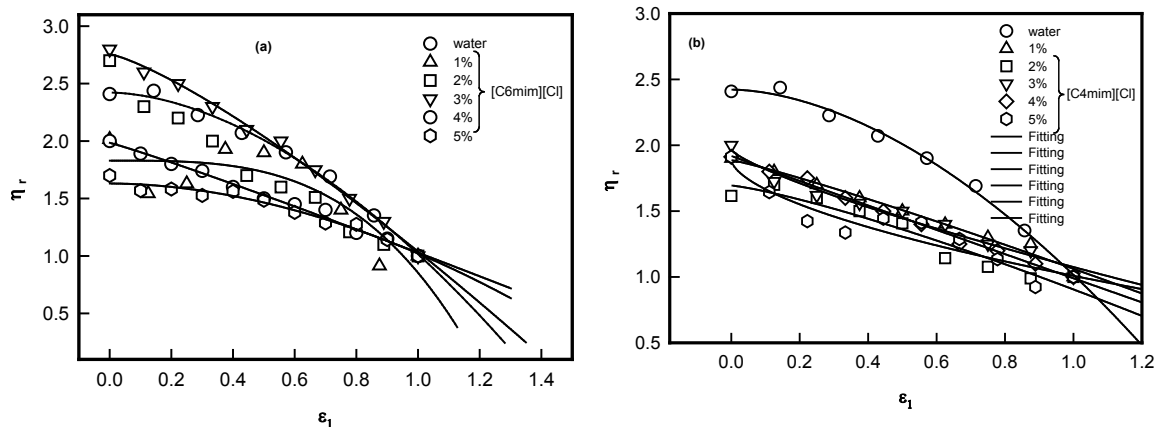


Figure S4: Relative viscosity data of a) [C6mim][Cl] and b) [C4mim][Cl] fitted to ϵ_1 using eq (4) that yielded power-law exponent, k (Table II). Solid line is the fitting curve to data points with Chi-squared > 0.95 . Standard deviations in the reported η values are ± 2 mPa s. See text for details.

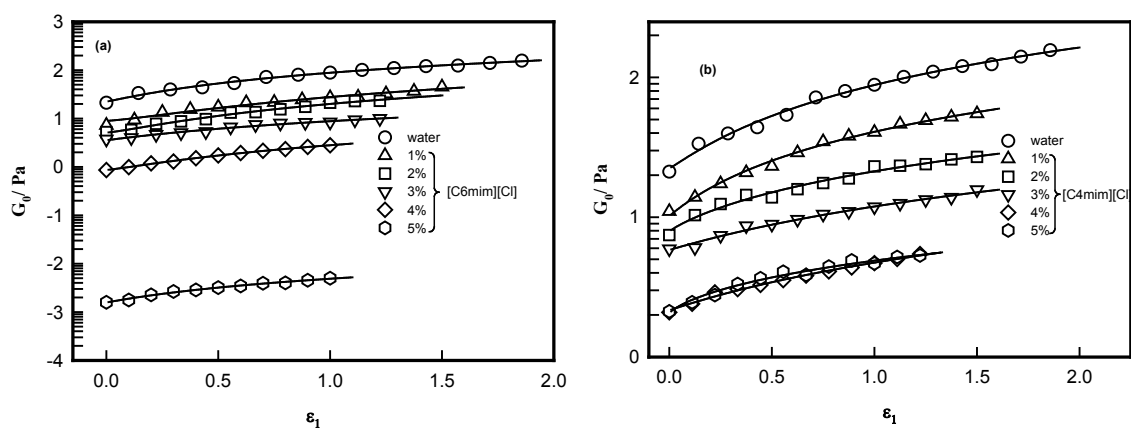


Figure S5: Low frequency storage moduli data of a) [C6mim][Cl] and b) [C4mim][Cl] fitted to ϵ_1 using eq (5) that yielded power-law exponents, t (Table II). Solid line is the fitting curve to data points with Chi-squared > 0.95 . See text for details. Standard deviations in the reported G_0 values are ± 2 Pa.

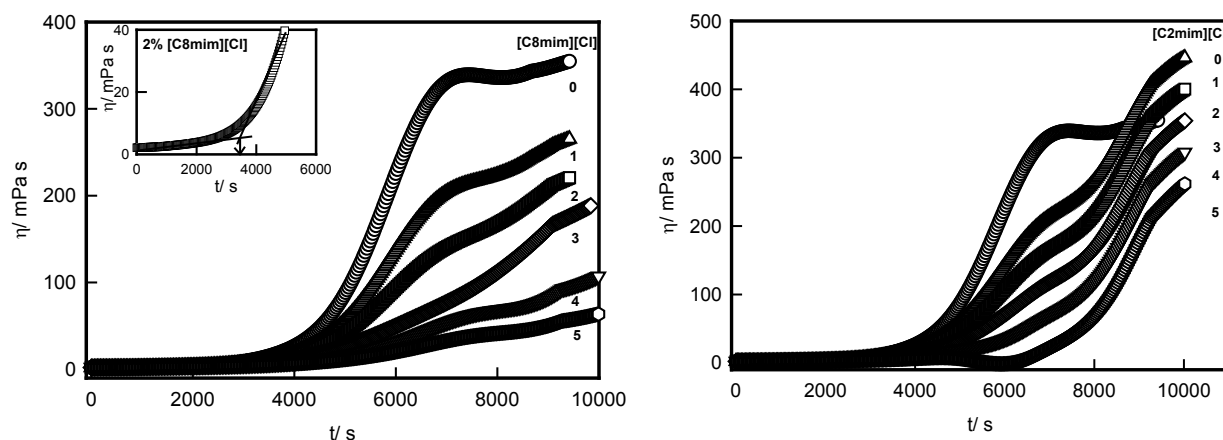


Figure S6: Time dependent viscosity plot of a) [C8mim][Cl] and b) [C2mim][Cl] based ionogels samples. Numbers mentioned on the curves represent IL concentration. The figure in inset shows the estimation of time of gelation (t_g). Standard deviations in the reported η and t values are ± 2 mPa s and ± 100 s.

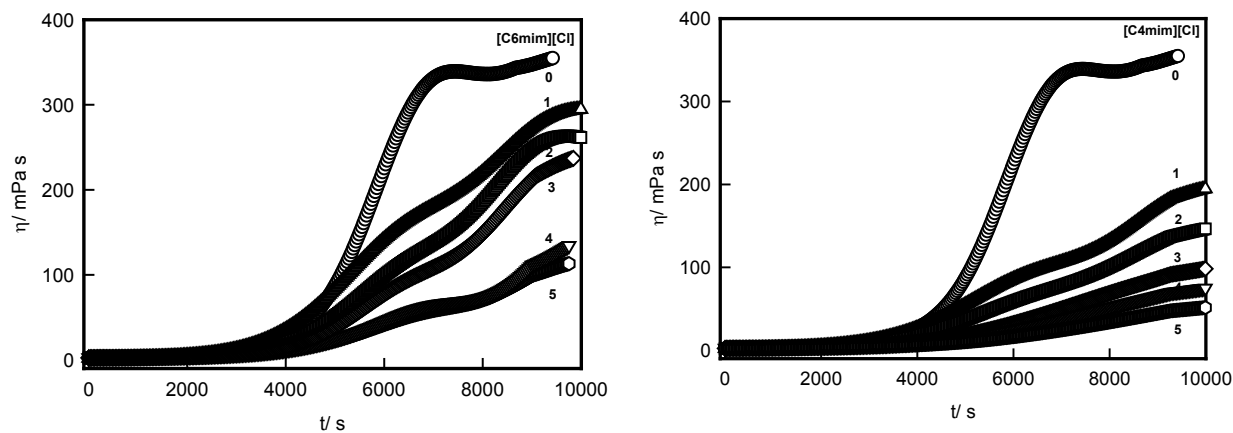


Figure S7: Time dependent viscosity plot of a) [C6mim][Cl] and b) [C4mim][Cl] based ionogels samples. Numbers mentioned on the curves represent IL concentration. Standard deviations in the reported η and t values are ± 2 mPa s and ± 100 s.

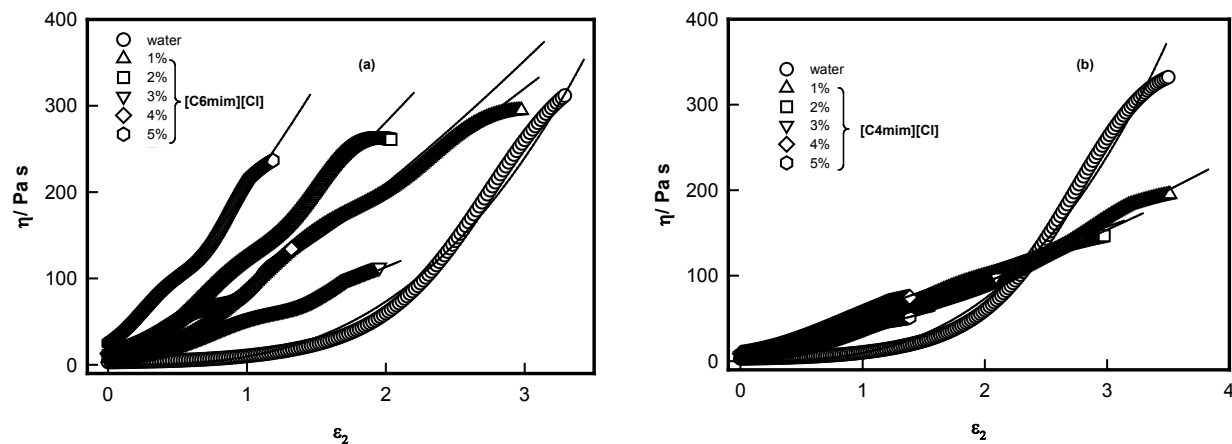


Figure S8: Viscosity data fitted to ϵ_2 of a) [C6mim][Cl] and b) [C4mim][Cl] using eq (9) that yielded power-law exponent, α (Table III). Solid line is the fitting curve to data points with Chi-squared > 0.95 . See text for details. Standard deviations in the reported η values are ± 2 mPa s.

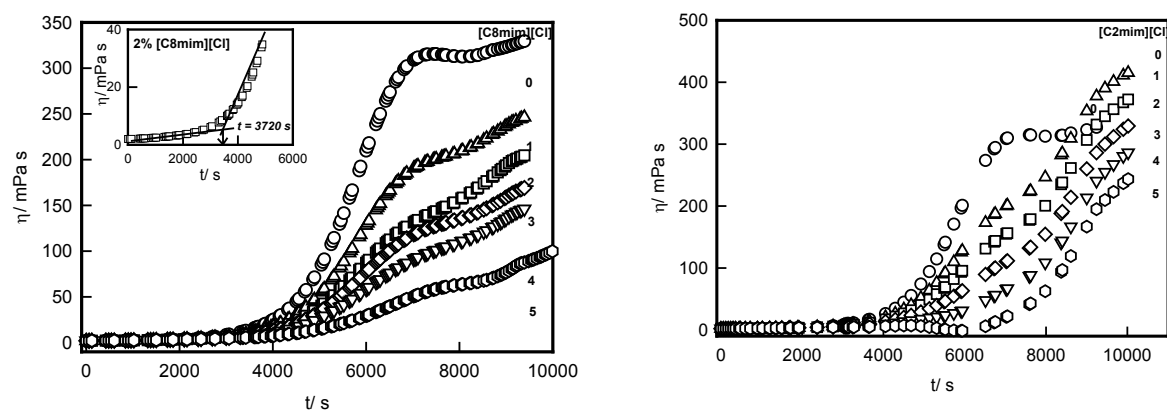


Figure S9: Time dependent hydrodynamic radius growth plot of a) [C8mim][Cl] and b) [C2mim][Cl] based ionogels samples. The figure in inset shows the estimation of time of gelation (t_g). Standard deviations in the reported R_h and t values are ± 5 nm and ± 100 s.

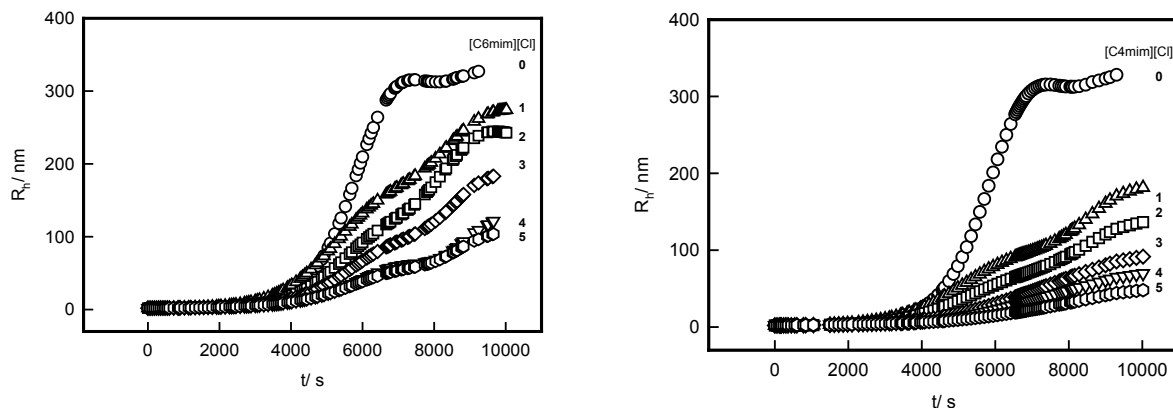


Figure S10: Time dependent hydrodynamic radius growth plot of a) [C6mim][Cl] and b) [C4mim][Cl] based ionogels. Numbers mentioned on the curves represent IL concentration. Standard deviations in the reported R_h and t values are ± 5 nm and ± 100 s.

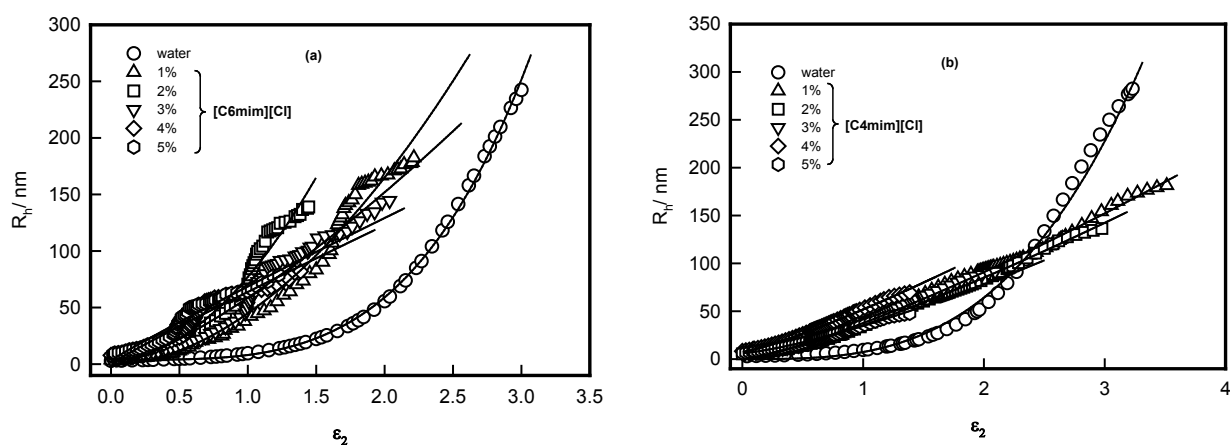


Figure S11: Hydrodynamic radii data fitted to ϵ_2 of a) [C6mim][Cl] and b) [C4mim][Cl] using eq (10) that yielded power-law exponent, β (Table III). Solid line is the fitting curve to data points with Chi-squared > 0.95 . See text for details. Standard deviations in the reported R_h data are ± 5 nm.